Measurement-Based On-Body Path Loss Modelling for UWB WBAN Communications

Timo Kumpuniemi, Tommi Tuovinen, Matti Hämäläinen, Kamya Yekeh Yazdandoost, Risto Vuohtoniemi, Jari Iinatti

Centre for Wireless Communications
University of Oulu
Oulu, Finland
{forename.surname}@ee.oulu.fi

***Abstract*—This paper presents a path loss model for an ultra wideband (UWB) wireless body area network (WBAN) on-body communication. The modelling is based on the static frequency domain measurements in an anechoic chamber. The studies are done for several on-body radio channels and with two different UWB antennas (dipole and double loop) for the frequency range of 2-8 GHz. A linear least squares (LS) polynomial data fitting is applied to the post processed measurement data resulting parameters for a path loss model. It is shown that the loop antenna outperforms the dipole antenna in respect to the slope of the attenuation. However, the path loss at the reference distance is higher for the loop. It is also shown that the signal propagation delay in the antenna structures causes error in distance measurement and unless the error is compensated significant differences in the parameters of the path loss model may occur in a WBAN case. Finally, it is observed that by using energy detection notable benefit can be obtained if all propagation paths are considered instead of the first arriving path.**

Keywords—body area network (BAN); path loss; ultra wideband (UWB).

I. INTRODUCTION

One result of the rapid development of wireless devices is that their size decreases constantly. This has eased up their usage close to the human body, even inside it [1]. Therefore these kinds of devices are extremely suitable for numerous applications in the area of health care. In recent years, a popular discussion topic has been ultra wideband (UWB) wireless body area network (WBAN) systems [1,2]. Wireless technologies enable to design different kinds of systems for on-body, in-body and off-body communications. The possibility of replacing wires when, e.g., monitoring the data measuring a patient's health widens the mobility, freedom and the quality of life of a patient into a totally new level. UWB signals are often defined to have the –3 dB bandwidth (BW) larger than 20% of their apparent center frequencies. On the other hand, UWB technology is also a highly suitable technology for short range communications needed in the medical BAN [3,4].

In 2012 the Institute of Electrical and Electronics Engineers (IEEE) published an international standard IEEE 802.15.6 for WBAN [5]. In the standard, UWB technology is defined to be used in the frequency ranges of 3.2448-4.7424 GHz (low band) and 6.24-10.2336 GHz (high band) with a channel BW of 499.2 MHz. Most probably the standard will speed up the activities in the UWB WBAN area into an even higher level.

This paper introduces a path loss model for UWB WBAN based on static measurements where the channel state is kept as constant as possible. A large number of on-body radio channels are examined by using frequency domain measurements with a vector network analyzer (VNA) in the frequency range of 2-8 GHz (VNA upper frequency limit is 8 GHz). The investigation is performed with two planar UWB antenna types: dipole and double loop. The measured data are post-processed to retrieve the time-domain results. The motivations for the examinations are to find out and compare the effect of different antenna types and to extract the influence of the distance error due to the antennas on the path loss modelling. The effect of detecting all arriving propagation paths instead of the first arriving one is also examined.

The structure of the paper is as follows. In Section II the measurement setup is described, in Section III the measurement scenarios are explained and Section IV contains the measurement results. In Section V conclusions and plans for the future work are given.

II. MEASUREMENT SETUP

A. Measurement Room and Test Person

The measurements were conducted in an anechoic chamber with a floor size of 245 cm by 365 cm and a height of 240 cm. The male test person had a height of 183 cm and he was wearing a cotton T-shirt, jeans and no shoes. All metal containing substances, e.g., ring, belt clasp and watch were removed for the measurements.

B. VNA Measurement Device and Antennas Under Test

The measurements were conducted by sweeping a frequency range of 2-8 GHz by using a VNA of the model Rohde & Schwarz ZVA8 with four test ports [6]. The Huber + Suhner SUCOFLEX 104PEA measurement cables had a length of 800 cm and a measured attenuation of 6.9-10.8 dB within the swept BW. The VNA was controlled with a laptop computer using LabVIEW software by National Instruments through the general purpose interface bus (GPIB) of the VNA. For each measured link, 100 consecutive sweeps each having 1601 points over the measured BW were recorded. As a result, the channel transmission coefficients corresponding to the scattering parameters S_{21} as a function of frequency were obtained. The sweep time of the VNA was 288.18 ms, the

978-1-4673-5772-2/13/$31.00 ©2013 IEEE

measurement BW, i.e., intermediate frequency (IF) BW was 100 kHz and the transmit power used was +10 dBm.

The structures and performances of the used UWB antennas, dipole and double loop, are presented in detail in [7-10] for the cheap, widely available, well-known FR4 substrate materials. Reference [11] includes the corresponding antenna figures with the TRF-43 antenna substrate, as those were used in this study. In Table I, the most important parameters of the measurement setup are gathered.

III. Measurement Scenarios

The measurement positions are shown in Fig. 1. Point A is placed either on-body on the abdomen or off-body on a pole. The points 4, 6, 8, 10 and 12 lie on the side of the body, arm or leg whereas the rest of the on-body spots are situated on their frontal parts. Since a 4-port VNA was used, four identical antennas were mounted simultaneously. In order to have a constant gap between the antennas and the body, a 20 mm thick piece of material called ROHACELL 31 HF [12] with similar electrical properties to air (ε_r = 1.05 @ 2.5 GHz, 1.043 @ 5 GHz, 1.046 @ 10 GHz) was used in the antenna-body gap. In practice, the antennas were fixed on the body by using elastic bands together with painter's masking tape. Fig. 2 shows an exemplary view of an antenna placement.

In total six combinations of four locations (sets) were chosen as listed in Table II. They all contained the point A while the other three spots were varied. The combinations were measured for both A being placed on the abdomen and on the pole. The links to/from the pole were excluded from the analysis since on-body links are the focus of this paper. The sets were mounted one-by-one for both antenna types and the frequency responses were measured. Then the measurements were repeated by re-mounting the antennas in order to reduce the effect of the variation of antenna positioning on the results.

IV. Measurement Results

The measured data were processed by using MATLAB software. In practice, an inverse fast Fourier transform (IFFT) was applied to the frequency domain data in order to extract the impulse responses of the measured links. No data windowing was used. The absolute values of the impulse responses were averaged over the 100 sweeps done for each link. From the average impulse responses the first arriving path was searched

TABLE I. Parameters of the Measurement Setup

Name of the Parameter	Parameter Value
Frequency band	from 2 to 8 GHz
VNA IF bandwidth	100 kHz
Number of points	1601
Sweep time	288.18 ms
Number of sweeps per link	100
Transmit power	+10 dBm
Measurement cable lengths	800 cm
Measurement cable loss at 2 GHz	6.9 dB
Measurement cable loss at 8 GHz	10.8 dB
Anechoic chamber floor size	245 cm by 365 cm
Anechoic chamber floor height	240 cm
Test person height	183 cm

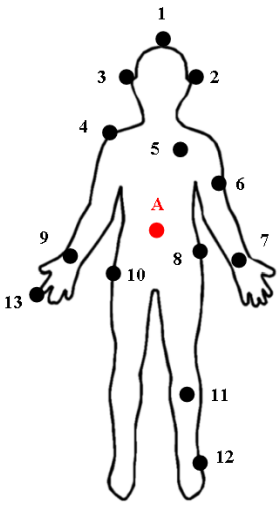

Figure 1. Measurement positions.

Figure 2. An exemplary view of the antenna placement at A – 5 – 6 – 7.

TABLE II. Combinations of Measurement Locations

A – 1 – 2 – 3	A – 10 – 11 – 12
A – 5 – 6 – 7	A – 4 – 9 – 13
A – 1 – 7 – 9	A – 4 – 8 – 10

and the delay and loss corresponding to the first path were found out. Based on the path delay the corresponding distance d_i was calculated by the well-known equation

$$d_i = c \cdot t, \tag{1}$$

where c is the velocity of the light in the air and t is the measured delay of the first arriving path.

This leads to an important aspect that is rarely commented in the articles in the field. Two methods can be used for the path loss derivation. The first one is to measure exactly the distance between the antennas before the measurements in order to know the path loss with this distance as is the case in classical channel modelling in longer link distances. The

second option is to find out the distance from the first peak in impulse response, which is the method used in this paper.

The first stage to start any VNA measurement is to calibrate the device. As a result, the zero time delay plane is transferred to the open ends of the measurement cables. I.e, if the cables were connected together a path delay of zero seconds would be measured. When antennas are connected to the cables the transmitted signal first has to pass the transmit antenna structure before entering into air. Since the antennas have some physical dimensions, the signal travelling through the antenna takes time causing an error in the path distance calculated based on (1). A second factor causing error is the fact that the velocity of the signal v in the antenna structures is [13]

$$v = \frac{c}{\sqrt{\varepsilon_r}}, \tag{2}$$

where ε_r is the relative permittivity of the medium in which the signal travels, i.e., the substrate for planar antennas. Thus the propagation speed v will be lower than c increasing the distance error. The error will occur both in transmit and receive antennas. Finally, this delay does not only depend on the physical dimensions and material of the antennas but also on the positions of the antennas relative to each other. In on-body radio channel measurements this error term may have a strong impact on the results in certain analyses. Since the link distances are generally very short in WBAN even an error term of a few centimeters may mean a large value in the error percentage. The case becomes more complicated when the exact path length of the channel is unknown as is the case for any signal path that does not have a line-of-sight (LOS) condition.

In order to compensate this error from the final results both antenna types were measured with a VNA by using a fixed 50 cm distance between the ends of the measurement cables. The antenna pairs (Antenna 1 and Antenna 2) were positioned vertically in open space and their positions in respect to each other were varied so that the reflector surfaces were first set towards each other (face-to-face) and measured. Next the antennas were rotated clockwise with several different angles. In total six different positions were measured as described in Table III. The angle for zero degrees describes the initial face-to-face position.

Table IV lists the obtained mean error and standard deviation results for the distance error measurement for both antenna types. As noted, the usage of loop antennas causes larger error in link distance than dipoles and the error is also more position dependent since the standard deviation is higher.

The obtained mean error values were used as correction parameters when defining the path length for each link described in Fig. 1 and Table II. In practice, the mean error was subtracted from all distance values d_i obtained from (1). The validity of the error correction factors were explicitly verified by comparing the error corrected distances with the distances measured on-body during the measurements. The obtained distances d were normalized by a reference distance of $d_0 = 50$ mm as was done in [14].

TABLE III. ANTENNA POSITIONS FOR DISTANCE ERROR MEASUREMENT

Position	Antenna 1	Antenna 2
1	0º	0º
2	90º	270º
3	270º	90º
4	270º	180º
5	180º	180º
6	0º	180º

TABLE IV. DISTANCE ERROR RESULTS

Antenna type	Mean error	Standard deviation
Dipole	90 mm	9.8 mm
Loop	109 mm	19.7 mm

The path loss model with distance dependency can be described by the equation [14-19]

$$PL(d) = PL(d_0) + 10n\log_{10}\left(\frac{d}{d_0}\right) + S \ \ [\text{dB}], \tag{3}$$

where PL is the path loss in dB, $PL(d_0)$ is the path loss at the reference distance, n is the path loss exponent and S is a random scattering term with standard deviation of σ around the mean value describing the effect of different on-body antenna positions and variation of antenna gains in different directions [15]. The path loss exponent in this paper is defined to be negative and in the case of free space it would reach the value of -2. The distances in the equation must obey the rule $d \geq d_0$.

Dipole Antennas

The measurement results for the various on-body radio links using dipole antennas are shown in Fig. 3. On the horizontal axis is the relative distance in logarithmic scale and the vertical axis shows the values of the path losses. Each dot on the figure represents one measured link and the averaged strength of its first arriving path component in decibels.

A linear least squares (LS) polynomial data fitting is applied to the data of the first arriving path to extract the parameter n in (3). This is shown as the red line in Fig. 3 and the slope of the line presents the obtained value of $n = -3.3$. This lies on the same levels that are reported in other on-body measurements [14,17,20,21] where typically values around -3 for links located mainly on frontal body are observed. However, the UWB BW is usually in these references narrower than in this paper or the investigations are performed in industrial, scientific and medical (ISM) non-UWB bands. The value for the path loss at the reference distance d_0 can be found to be $PL(d_0) = -31.6$ dB. This value can be noted to be higher as reported in [16] but less than the corresponding value in [20] taking into consideration that in [20] $d_0 = 10$ cm.

The average path loss is worked out as the mean of linear valued path losses giving the decibel scaled result of -57.6 dB. When examining a certain single distance the variation of the obtained path loss can be noted to be quite high. The standard deviation of path losses in decibels in Fig. 3 is $\sigma = 12.8$ dB. This value is larger than usually reported in the published articles in the field but can be explained by the differences of

the measured links. Consider for instance the measurement location combination A – 4 – 8 – 10 in Fig. 1 and Table II. The position 4 is on the right shoulder while the point 8 is approx. 10 cm above the left hip. Therefore they lie on the different sides of the body and no LOS path exists. As a result, a large path loss for these cases is intelligible. If then, e.g., the location combination A – 5 – 6 – 7 is considered as in Fig. 2, the signal paths can be understood to be significantly better when the path loss is examined. Approximately similar link distances as in link 4 – 8 are available but the path loss is considerably lower. As a result a high value of σ is obtained.

From the measurement data also a result which sums together all received signal samples with propagation path lengths less than 1.6 m. The data fitting for that is shown with the black dashed line in Fig. 3. It can be noted that now n = −3.1 giving a result that the first arriving path dominates the impulse response since the difference between the n of the first path case is quite small. The level of the fitting line of the summed paths is approx. 12.6-14.2 dB higher than the line for the first path. Therefore if an energy detector would be used in the receiver, a gain similar to these values could be obtained by receiving all the paths. If then, e.g., the –60 dB level in Fig. 3 is assumed to be the a minimum level for detection, it can be noted that by receiving all signals paths with the length below 1.6 m instead of the first path, a four-fold operation distance can be reached. All path loss model results are collected together in Table V.

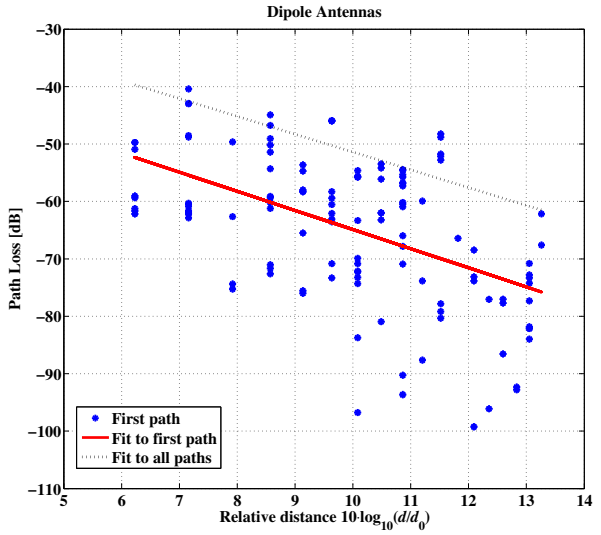

Figure 3. Measurement results with the dipole antennas.

TABLE V. PATH LOSS MODEL PARAMETERS WITH ERROR CORRECTION

	First Path		All Paths	
Parameter	***Dipole***	***Loop***	***Dipole***	***Loop***
n	−3.3	−2.7	−3.1	−2.6
d_0	50 mm	50 mm	50 mm	50 mm
$PL(d_0)$	−31.6 dB	−39.8 dB	−20.4 dB	−25.1 dB
Average Path Loss	−57.6 dB	−58.9 dB	−44.4 dB	−44.3 dB
σ	12.8 dB	13.8 dB	11.6 dB	12.2 dB

Double Loop Antennas

The analysis results for the double loop antenna are shown in Fig. 4. The measured links are identical to the ones in the case of dipoles excluding the natural small variation in the antennas' on-body mounting locations. After processing the data as above, a slope factor of n = −2.7 was obtained for the first path analysis. This is clearly a smaller value than for the dipole. The result for the path loss at the reference distance d_0 can be found to be $PL(d_0)$ = −39.8 dB which is considerably higher than for the dipole case. The average path loss for loops is found to be −58.9 dB and the standard deviation of the path loss is σ = 13.8 dB, i.e., a value of 1 dB higher than for the dipoles and therefore giving a slightly weaker performance for loops in this sense. An analysis for the summed signal paths with distances under 1.6 m is done as for dipoles, and the same kind of observations can be made for the loop also.

Based on the results for the two antenna types, it can be stated as a general observation that the signal seems to decay faster for the dipoles but the values for the attenuation at reference distance, average path loss and standard deviation of the path loss show weaker performance for the loop antennas.

When comparing the results with those presented in other articles the results correspond with many of them taking into account the fact that the on-body links considered in those are far more homogenous than the ones examined in this study. This has certain effects on the results, e.g., the higher value of standard deviation.

As discussed above, the error caused by propagation delay in antennas may have in some cases a strong effect on the results in short (such as WBAN) distances. To verify this, the data analysis was repeated for uncorrected distance values and the results are shown in Table VI. As noted, the uncorrected distance values produce highly different parameters for (3). The slope factor n for attenuation is clearly higher as is the case with the parameter values $PL(d_0)$. The rest of the parameters in the Table VI remain the same compared to Table V.

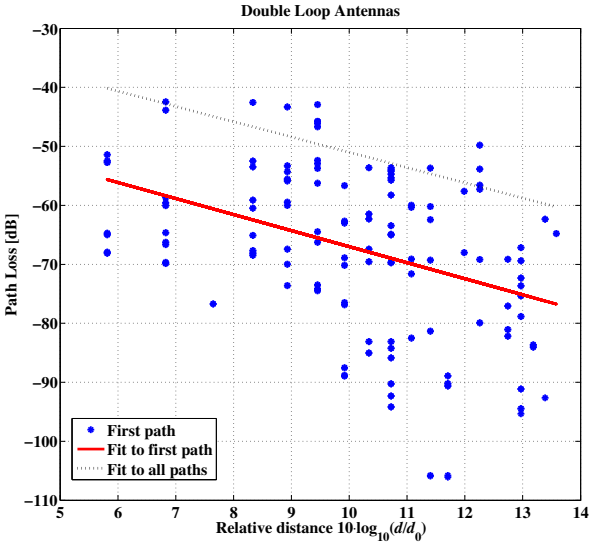

Figure 4. Measurement results with the double loop antennas.

TABLE VI. PATH LOSS MODEL PARAMETERS WITHOUT ERROR CORRECTION

	First Path		All Paths	
Parameter	***Dipole***	***Loop***	***Dipole***	***Loop***
n	−4.0	−3.4	−3.8	−3.3
d_0	50 mm	50 mm	50 mm	50 mm
$PL(d_0)$	−21.4 dB	−29.5 dB	−10.8 dB	−15.1 dB
Average Path Loss	−57.6 dB	−58.9 dB	−44.4dB	−44.3 dB
σ	12.8 dB	13.8 dB	11.6 dB	12.2 dB

V. CONCLUSIONS AND FUTURE WORK

In this paper, a path loss model for UWB on-body WBAN is introduced. The model is based on static frequency domain measurements in an anechoic chamber with a VNA in the frequency range of 2-8 GHz. The investigation is performed with two UWB antenna types: dipole and double loop. The measured data was post-processed in order to solve the corresponding time-domain impulse responses. For the analyses, the impulse responses were examined first by finding the strength and time delay of the first arriving path. Secondly, all signals with propagation path lengths under 1.6 meters were integrated together.

It was shown that on the average the loop antenna outperforms the dipole antenna in respect to slope of the attenuation. However, the results for the attenuation at the reference distance, average path loss and the standard deviation of the path loss are noted to be better for the dipole. Energy detection was found to be beneficial compared to the first path detection. It was also noted that the signal propagation delay in the antenna structures causes error in distance measurement. Unless this error is compensated, significant differences in the parameters of the path loss model may occur.

Examination of the existing large amount of the measurement data further to verify the reasons behind the differences in the path loss models between the two antennas will be one of the next steps of the work. Also an extension to pseudo-dynamic or even dynamic channel measurements will be interesting topics for the future work.

ACKNOWLEDGMENTS

This work has been partly funded by the Finnish Funding Agency for Technology and Innovation (Tekes) through the project Wireless Body Area Network for Health and Medical Care (WiBAN-HAM).

The authors wish to thank Mr. Veikko Hovinen from the Centre for Wireless Communications for fruitful discussions.

REFERENCES

[1] P. S. Hall, and Y. Hao, Antennas and Propagation for Body-Centric Wireless Communications. Norwood, MA: Artech House, 2012, 2nd ed., pp. 1-16 and 139-160.

[2] A. Fort, C. Desset, P. De Doncker, P. Wambacq and L. Van Biesen, ''An ultra-wideband body area propagation channel model—from statistics to implementation," IEEE Trans. Microw. Theory Tech., vol. 54, pp. 1820-1826, Apr 2006.

[3] I. Oppermann, M. Hämäläinen, J. Iinatti (eds.), UWB Theory and Applications. West Sussex, England, John Wiley & Sons, 2004, pp. 1-7.

[4] D. Cassioli, M. Z. Win, A. F. Molisch, "The ultra-wide bandwidth indoor channel: from statistical model to simulations," IEEE J. Sel. Areas Commun., vol. 20, pp. 1247-1257, Aug. 2002.

[5] IEEE standard for local and metropolitan area networks, IEEE 802.15.6-2012 – Part 15.6: wireless body area networks, 2012.

[6] Rohde & Schwarz (accessed in November 2012), [Online]. Available: http://www2.rohde-schwarz.com/en/products/test_and_measurement/network_analysis/ZVA8_%284-Port%29.html.

[7] T. Tuovinen, M. Berg, K. Yekeh Yazdandoost, E. Salonen, and J. Iinatti, "Reactive near-field region radiation of planar UWB antennas close to a dispersive tissue model," In Proc. Loughborough Antennas Propag. Conf. (LAPC), Nov. 2012, United Kingdom.

[8] T. Tuovinen, M. Berg, K. Yekeh Yazdandoost, E. Salonen, and J. Iinatti, "Impedance behaviour of planar UWB antennas in the vicinity of a dispersive tissue model," In Proc. Loughborough Antennas Propag. Conf. (LAPC), Nov. 2012, United Kingdom.

[9] M. Särestöniemi, T. Tuovinen, M. Hämäläinen, K. Yekeh Yazdandoost, and J. Iinatti, "Channel modeling for UWB WBAN on-off body communication link with finite integration technique," In Proc. 7th Int. Conf. on BANs (BodyNets), Sep. 2012, Oslo, Norway, pp. 1-7.

[10] T. Tuovinen, K. Yekeh Yazdandoost, and J. Iinatti, "Comparison of the performance of the two different UWB antennas for the use in WBAN On-Body Communications," In Proc. 6th Europ. Conf. Antennas Propagat. (EuCAP), March 2012, Prague, Czech, pp. 3371-3374.

[11] T. Tuovinen, T. Kumpuniemi, K. Yekeh Yazdandoost, Matti Hämäläinen, Jari Iinatti, "Effect of the antenna-human body distance on the antenna matching in UWB WBAN applications", 7th Int. Symp. Medical Inform. and Commun. Technol. (ISMICT 2013), in press.

[12] Rohacell (accessed in November 2012), [Online]. Available: http://www.rohacell.com/product/rohacell/en/products-services/rohacell-hf/pages/default.aspx.

[13] D. M. Pozar, Microwave Engineering, Third Edition. Danvers, MA: John Wiley & Sons Inc., 2005, pp.1-161.

[14] K. Yekeh Yazdandoost, K. Sayrafian-Pour, and K. Hamaguchi, "RF propagation and channel modeling for UWB wearable devices," IEICE Trans. Commun., vol. E94-B, no. 5, pp. 1126-1134, May 2011.

[15] K. Sayrafian-Pour; W.-B. Yang; J. Hagedorn; J. Terrill; K. Yekeh Yazdandoost, "A statistical path loss model for medical implant communication channels," In Proc. IEEE 20th International Symposium on Personal, Indoor and Mobile Radio Communications (PIMRC), Sept. 2009, Tokyo, Japan, pp. 2995 - 2999.

[16] H. Viittala, M. Hämäläinen, J. Iinatti, A. Taparugssanagorn, " Different experimental WBAN channel models and IEEE802.15.6 models: comparison and effects," In Proc. 2nd International Symposium on Applied Sciences in Biomedical and Communication Technologies, (ISABEL), November 2009, Bratislava, Slovak Republic.

[17] A. Taparugssanagorn, A. Rabbachin, M. Hämäläinen, J. Saloranta and J. Iinatti, "A review of channel modelling for wireless body area network in wireless medical communications" In Proc. 11th International Symposium on Wireless Personal Multimedia Communications (WPMC), Aug. 2008, Lapland, Finland.

[18] K. Yekeh Yazdandoost, K. Sayrafian-Pour., "Channel model for body area network (BAN)," IEEE P802.15 working group for wireless personal area networks (WPANs) (IEEE P802.15-08-0780-12-0006, 10 Nov. 2010).

[19] A. F. Molisch et al., "IEEE 802.15.4a channel model-final report," IEEEP802.15 working group for wireless personal area networks (WPANs) (IEEE 802.15-04-0662-01-04a, Sept. 2004).

[20] A. Fort, C. Desset, J. Ryckaert, P. De Doncker, L. Van Biesen, and P. Wambacq, "Characterization of the ultra wideband body area propagation channel," in Proc. ICU IEEE International Conference, Sept. 2005, Zurich, Switzerland, pp. 22-27.

[21] E. Reusens, W. Joseph, B. Latré, B. Braem, G. Vermeeren, E. Tanghe, L. Martens, I. Moerman and C. Blondia, "Characterization of on-body communication channel and energy efficient topology design for wireless body area networks," IEEE Trans. Inf. Technol. Biomed., vol. 13, pp. 933-945, Nov. 2009.